Oxidative dehydrogenation of propane with cobalt, tungsten and molybdenum based materials

Deshidrogenación oxidativa de propano con materiales a base de cobalto, tungsteno y molibdeno

Maurin Salamanca-Guzmán[1, 2*], **Yordy Enrique Licea-Fonseca**[3], **Adriana Echavarría-Isaza**[1], **Arnaldo Faro**[4], **Luz Amparo Palacio-Santos**[5]

[1] Grupo Catalizadores y Adsorbentes, Instituto de Química, Universidad de Antioquia. Calle 67 # 53-108. A. A. 1226. Medellín, Colombia.

[2] Department of Chemistry, Bielefeld University. Universitätsstraße 25, D-33501. Bielefeld, Germany.

[3] CENANO-DCAP, Instituto Nacional de Tecnologia. Av. Venezuela 82. CEP 20081-312. Rio de Janeiro, Brasil

[4] Departamento de Físico-Química, Instituto de Química, Universidade Federal do Rio de Janeiro. Av. Athos da Silveira Ramos, 149. CEP 21941-909. Río de Janeiro, Brasil.

[5] Departamento de Operações e Processos Industriais, Instituto de Química, Universidade do Estado do Rio de Janeiro. Rua São Francisco Xavier, 524. CEP 20550-900. Río de Janeiro, Brasil.

ABSTRACT: Oxidative dehydrogenation of propane is a reliable alternative for olefins production. This paper presents the results obtained on oxidative dehydrogenation of propane by using two materials based on cobalt, tungsten, and molybdenum. The materials were characterized by X-ray diffraction (XRD), Fourier transform infrared spectroscopy (FTIR), temperature programmed reduction (TPR), thermogravimetric analysis (TGA), and differential thermal analysis (DTA). The CoMoϕy material was calcined at 623 K, transforming itself to β-CoMoO4 phase (CoMoϕ623), the same phase is observed when the material is calcined at 873 K (CoMoϕy873). CoMoϕy623 showed the best performance in oxidative dehydrogenation of propane, a yield to propene of 3.4% was obtained at 623 K using a space velocity of 100 mLg-1min-1. CoWsϕy was calcined at 673 K, a low crystallinity wolframite was obtained. This material has a high selectivity to propene and low yield. CoMoϕy873 has a selectivity and conversion within the range of the results reported in the literature. This is a prospective catalyst for the oxidative dehydrogenation of propane; it was stable for 24 h of continuous operation at 773 K.

RESUMEN: La deshidrogenación oxidativa de propano es una alternativa interesante para la obtención de olefinas. En este trabajo se presentan los resultados obtenidos en la deshidrogenación oxidativa de propano utilizando dos materiales a partir de cobalto, tungsteno y molibdeno. Los materiales fueron caracterizados utilizando Difracción de Rayos X (XRD), espectroscopia infrarroja con transformada de Fourier (FTIR), análisis termogravimétrico (TGA) y análisis térmico diferencial (DTA). El material CoMoϕy al ser calcinado a 623 K se transforma en la fase β-CoMoO4 (CoMoϕy623), la misma fase es obtenida cuando el material se calcina a 873 K (CoMoϕy873). CoMoϕy623 muestra un buen desempeño en la deshidrogenación oxidativa de propano, se obtuvo un rendimiento a propeno de 3,4% a una temperatura de 623 K y una velocidad espacial de 100 mL g-1 min-1. El material CoWsϕy fue calcinado a 673 K, obteniéndose una fase wolframita de baja cristalinidad. Este material presenta una alta selectividad a propeno y un bajo rendimiento. CoMoϕy873 presenta una buena actividad y selectividad, comparable con otros materiales reportados en la literatura, y su potencial como catalizador en la deshidrogenación oxidativa de propano se hace más evidente con la prueba que muestra ser estable durante 24 h de operación continua a 773 K.

1. Introduction

Alkenes or olefins are traditionally obtained in oil refineries, either from natural gas through extraction processes, or by fluidized bed naphtha catalytic steam cracking. However, due to the constant growth in consumption of olefins and derivatives in the world market, these methods are insufficient. Thus, different synthesis paths to light olefins (C2-C4) production have been studied [1]. The dehydrogenation process offers the possibility to obtain olefins, and it requires high temperatures (>873 K). This condition can generate problems due to thermal cracking side reactions and fast and continuous coke formation; it can imply a total loss of the catalytic activity due to irreversible deactivation or a regeneration step of the catalyst [2].

To overcome the disadvantages of the alkane dehydrogenation process, several alternatives have been proposed, such as the development of catalysts with a higher selectivity and resistance to deactivation or coupling the dehydrogenation reaction (endothermal) with methane oxidation (highly exothermal), to provide the heat required for the dehydrogenation and shift the balance towards alkenes [3]. Nevertheless, the alternative that has aroused more interest is the oxidative dehydrogenation, using oxygen in the reaction mixture to generate olefins, without side or consecutive reactions. In the oxidative dehydrogenation, thermodynamic limitations are overcome, allowing milder operating conditions and avoiding the need for continuous catalyst regeneration. However, the main difficulty is to avoid the consecutive total oxidation to carbon oxides from the light alkane, implying the need for the development of materials with high selectivity [4].

Transition metal oxides are recognized as the best catalysts for oxidative dehydrogenation. Molybdenum, vanadium and cobalt oxides show catalytic activity from 473 K [5]. Vanadium pentoxide is the most studied system. It does not present catalytic activity as a bulk material; the selectivity to propene obtained with supported V_2O_5 systems is between 60 and 80% and conversions about 1-15% [6–9]. The performance of niobium compounds is similar to that observed with vanadium compounds [10, 11].

Molybdenum compounds have shown low catalytic activity; nevertheless, different molybdates, such as $NiMoO_4$, have higher conversions than those obtained with vanadium-based materials, with a lower selectivity [12–14]. Additionally, transition metal mixed oxides of Mo, V, Fe, Co, Ce, Mn, Te have been studied before, and they have shown a good catalytic activity in oxidative dehydrogenation [15–17].

Tungsten-based materials have not been extensively studied in this particular reaction. Mo-W and V-W mixed oxides supported on alumina or silica have been studied providing good selectivity results but not good conversion [18, 19]. Different catalytic systems for oxidative dehydrogenation of propane based on Co and Ni molybdates or tungstates have been tested; these systems showed a good selectivity and a promising propene yield [20, 21].

In this work, bulk materials in Co-Mo and Co-W systems have been synthesized, which are promising as catalytic precursors in oxidative dehydrogenation of propane. The conditions for a good catalytic performance were found, taking into account parameters such as selectivity, conversion, and stability.

2. Experimental

2.1. Catalysts preparation

Bimetallic precursors were prepared using a co-precipitation method and were denominated CoMoφy and CoWsφy. The synthesis was carried out by preparing solutions of the metal salts, which were mixed and homogenized during the required time to form the gel. The salts used were $Co(NO_3)_2 \cdot 6H_2O$ (Merk), $(NH_4)_6Mo_7O_{24} \cdot 4H_2O$ (Merk) and WO_3 (Aldrich); tungsten oxide was dissolved with NH_4OH, the NH_4OH was also used as the precipitating agent. Next, the precipitating agent was added to the mixture, which was allowed to crystallize for 4 h at 353 K. In the end, the solids were recovered by filtration. Table 1 shows the molar gel composition of the precursor materials. The precursors were dried in a convection oven at 373 K. The final catalyst was obtained from calcination of the precursors at the temperatures that were chosen based on the thermal behavior shown below. Calcination temperature was defined at 673 K for CoWsφy and at 623 K for CoMoφy.

Table 1 Molar gel composition for the synthesized precursors

Precursor	Gel molar composition
CoMoφy	$MoO_3 : Co(NO_3)_2 : 3\ NH_4OH : 186\ H_2O$
CoWsφy	$WO_3 : Co(NO_3)_2 : 3.8\ NH_4OH : 190\ H_2O$

Hereafter, the precursors or fresh materials are denominated CoMoφy and CoWsφy. The catalysts were denominated with the name of the precursor plus the calcination temperature: CoMoφy623 and CoWsφy673.

2.2. Materials characterization

X-Ray diffraction was carried out in a Miniflex model Rigaku equipment with Cu source (λ= 1,5418 Å) operated at 40 kV and 30 mA for values between 5 and 40° and with scanning rate 2° min^{-1}. The thermal stability of the materials was studied by thermogravimetric analysis (TGA) and differential thermal analysis (DTA). TGA was carried out in TA Instruments Hi-Res TGA 2920 in a temperature range between 303 K and 1073 K, at a 10 K min^{-1} heating rate, under inert atmosphere (N_2) and DTA was carried-out on a TA Instruments DSC 2920 model using the same conditions as in TGA. Additionally, fourier transform infrared (FTIR) spectra were obtained with a Perkin Elmer Spectrum One equipment. The samples were prepared as wafers containing ~1 wt% sample in KBr. Moreover, the temperature-programmed reduction (TPR) analyses was performed in a Zeton Altamira AMI-70; in this case, the pre-treatment was carried-out by heating the sample (50mg) from room temperature to 573 K under argon atmosphere, and the

catalyst reduction took place under a 30 mL min^{-1} flow of H$_2$ (10 vol %)/Ar mixture, raising the temperature from room temperature to 1273 K at 10 K min^{-1}.

2.3. Catalytic tests

Oxidative dehydrogenation of propane was performed in a quartz reactor, using a propane to oxygen molar ratio of 2:1 in the reactant mixture. Temperatures in the range 473-873 K were used, 0.4 g of catalyst and a space velocity of 50 mL.g^{-1}.min^{-1} (298 K and 1 atm) were used. For the catalyst that showed the best performance, different space velocities were tested. During each reaction, the effluent of the reactor was analyzed in a Shimadzu GC-9A gas chromatograph equipped with TCD detector and Molecular Sieve 5A and Porapack Q columns. Calculations of conversion, selectivity, and yield of the reaction for each catalyst were carried out. The main products were propene, CO$_2$ and CO, and some traces of CH$_4$ and C$_2$H$_4$.

3. Results and discussion

3.1. Characterization
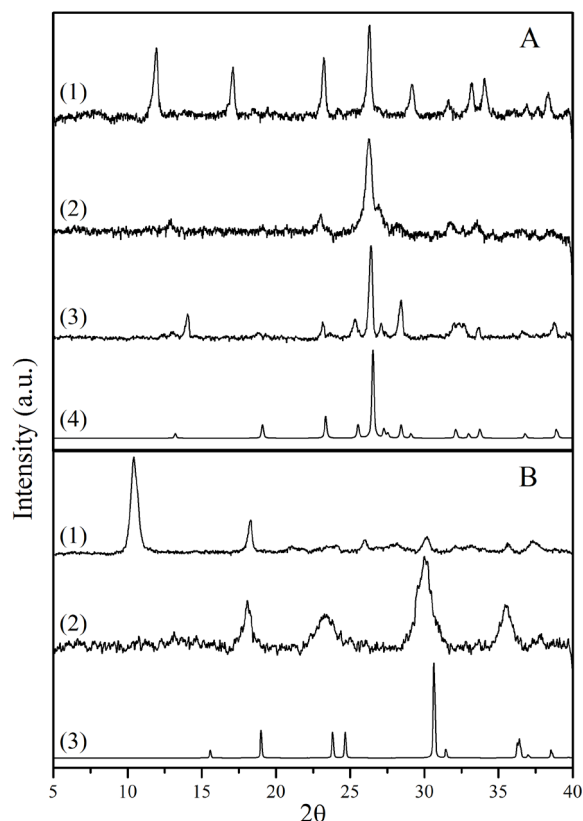
X-ray diffraction (XRD)

Figure 1 XRD patterns for A: (1) CoMoφy, (2) CoMoφy calcined at 623K, (3) CoMoφy calcined at 873K, (4) *β*-CoMoO$_4$ pattern. B: (1) CoWsφy, (2) CoWsφy calcined at 673K, (3) CoWO$_4$ pattern

φy phase assignation for the material denominated CoMoφy, Figure 1(a), was performed through comparison between the obtained diffractogram and the one reported by Pezerat [22] and Levin *et al.* [23]. The diffractogram for CoMoφy calcined at 623 K corresponds to ß-CoMoO$_4$ phase, which has been previously reported by Smith [24] also in agreement with the pattern of the Powder Diffraction File (PDF 21-868) database. According to literature, this phase is stable at high temperatures; therefore, no changes are expected in the structure of the material at temperatures above 623 K. The material denominated CoWsφy apparently is a semi-crystalline phase or a phase in formation process, Figure 1(b). When this material is calcined, a low crystalline wolframite-type cobalt tungstate (PDF 72-0479) is obtained.

Thermal analysis (TA)

For CoMoφy, Figure 2(a), a weight loss of 11.9% is observed between 373 K and 623 K, which corresponds to two exothermic events related to the evolution of volatile species from the lamellar solid, crystallization water and ammonia, the latter present in the structure as balance cation. In contrast, with CoWsφy (Figure 2(b)), an apparent single event between 373 K and 673 K is observed, with a weight loss of 5.6%. However, a shoulder is observed at 570 K, the main event at 608 K is assigned to the evolution of crystallization water, and the shoulder is related to a lower amount of ammonium cation present in the CoWsφy structure. The highest temperatures at which materials no longer present thermal events are 623 K for CoMoφy and 673 K for CoWsφy. For this reason, these temperatures were set as calcination temperatures to obtain the final catalysts.
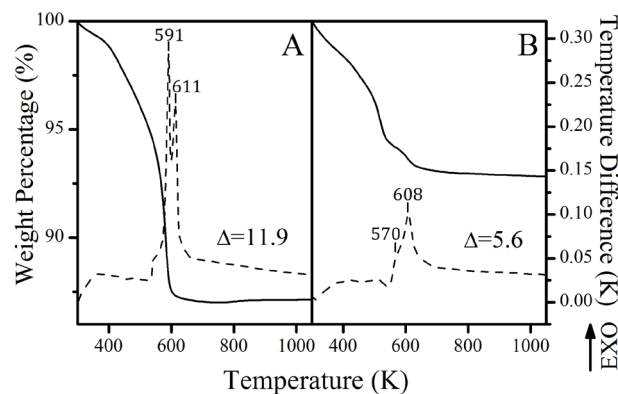
Figure 2 Thermal analysis for (A) CoMoφy (B) CoWsφy. Solid lines represent the thermogravimetric analysis (TGA), dash lines represent the differential thermal analysis (DTA)

Temperature programmed reduction (TPR)

The TPR profiles for the calcined materials are presented in Figure 3. For CoMoφy623 consistency with the reduction temperatures reported by Brito and Barbosa [25] for *β*-CoMoO$_4$ were observed. It was established that a reduction to lower valence oxidized states takes place, generating

equimolar mixtures of $Co_2Mo_3O_8$ and Co_2MoO_4 species, followed by a high-temperature reduction to the metals; these events take place at 807 K and 1113 K respectively. Additionally, a shoulder at 973 K is observed, which can be attributed to the reduction of an amorphous phase impurity obtained when calcination of the lamellar precursor took place. This amorphous phase was not observed by X-ray diffraction.

For CoWsφy673 the reduction events are observed from 673 K upwards, with two peaks at 1073 K, and 1123 K. Complete reduction of the material is achieved at temperatures near 1173 K. This profile is common for tungsten oxide catalysts, which present reduction at temperatures higher than 1073 K [26].
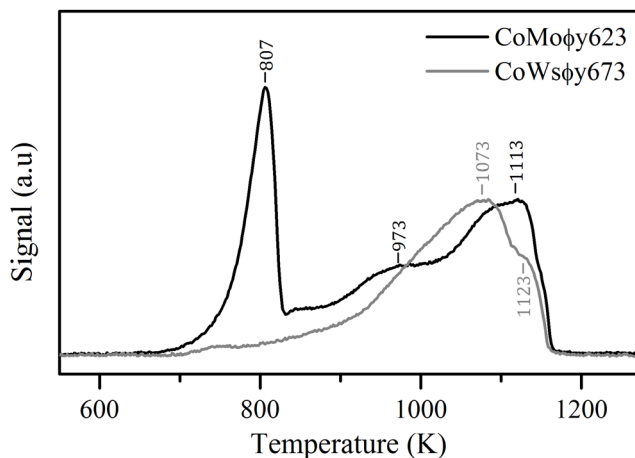

Figure 3 TPR profiles for CoMoφy623 and CoWsφy673 by reduction with 10% H_2/Ar mixture, from room temperature to 1273 K at 10 K min^{-1}

Fourier transform infrared spectroscopy (FT-IR)

Infrared spectra were obtained for the precursors and the calcined materials (Figure 4). For CoMoφy, bands at 928 and 620 cm^{-1} are associated with symmetric O-Mo-O stretching vibrations; the bands at 865, 806, 751 and 475 cm^{-1} correspond to asymmetric O-Mo-O stretching. All the bands correspond to characteristic vibration modes MoO_4^{2-} tetrahedra. For CoMoφy623, bands at 943, 841, 784, 704 and 418 cm^{-1} are observed, which correspond to the vibration bands of ß-CoMoO$_4$ structure [27]. This confirms the XRD results, cf. Figure 1.(b).

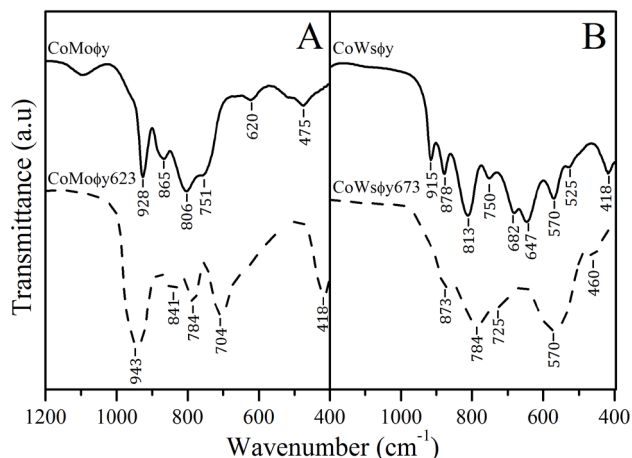**Figure 4** Infrared spectra of the precursors and the calcined materials (A) CoMoφy and (B) CoWsφy. Solid lines precursors, dash line calcined materials

In CoWsφy spectra, bands at 915, 813 and 418 cm^{-1} are observed, which agree with the vibration bands observed for scheelite-type oxides, where tungsten is in tetrahedral coordination. Meanwhile, the band at 878 cm^{-1} is related to symmetric vibration, and the bands at 750, 682, 647, 570 and 525 cm^{-1} are related to the asymmetric wolframite-type oxide vibrations, where the tungsten has octahedral coordination [28, 29]. For CoWsφy673, there is a good agreement with the reported information for wolframite [30], indicating octahedral coordination of cobalt and tungsten. The band at 873 cm^{-1} is related with WO_6^{6-} octahedra symmetrical stretching, while the bands at 784, 725 and 570 cm^{-1} are related with asymmetric stretching of the same group; the band at 460 cm^{-1} corresponds to the bending of it. The deformation of the spectra is caused by the low crystallinity of the solid observed in the XRD pattern, Figure 1(b).

Catalytic tests

Figure 5(a) shows that CoMoφy623 has a measurable catalytic activity from 523 K and CoWsφy673 from 573 K. The propane conversions are relatively high (Figure 5(a)), taking into account the low temperatures at which catalytic activity was evaluated. The catalyst that presented the best performance, regarding conversion, was CoMoφy623, with 18.5% conversion at 623 K, while CoWsφy673 reached conversions smaller than 10% even at 673 K. However, selectivity (Figure 5(b)) at 623 K presents an inverse behavior to that observed with the conversion. Selectivity to propene for CoMoφy623 tends to be stable at temperatures above 573 K, with a value close to 27%.
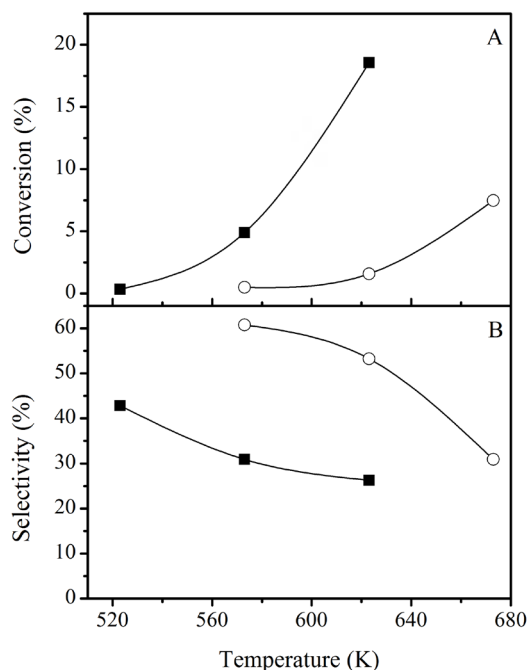
Figure 5 (A) Propane conversion and (B) selectivity to propene as a function of the temperature with a space velocity of 50 mLg⁻¹min⁻¹. CoMoφy623 (-■-), CoWsφy673 (-○-)

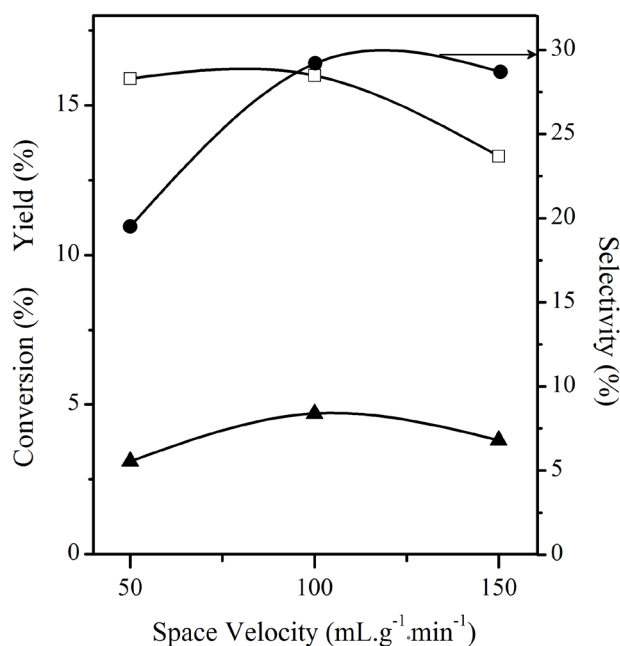Figure 1(a), did not show any significant changes in the structure, and it also corresponds to β-CoMoO$_4$.

Figure 6 Dependence on conversion (-□-), yield to propene (-▲-) and selectivity to propene (-●-) with space velocity for CoMoφy623 at 623 K

In order to explore CoMoφy623 as a catalyst, the reaction temperature was fixed at 623 K, and the space velocity was tested between 50 and 150 mL g⁻¹ min⁻¹. The results are shown in Figure 6. A high space velocity could avoid a total occupancy of the active sites available in the catalyst. Therefore, the conversion could be low. Lower space velocity implies longer contact time; this can increase the conversion and the side reactions. For CoMoφy, the best yield at 623 K was obtained at a space velocity of 100 mL g⁻¹ min⁻¹. Then, higher temperatures were used to increase the conversion. For this purpose, the precursor material CoMoφy was calcined at a higher temperature (873 K) and denominated CoMoφy873. The XRD pattern for CoMoφy873,

Conversion and selectivity values obtained with CoMoφy623 and CoMoφy873, at 100 mLg⁻¹min⁻¹ space velocity to different temperatures, are shown in Table 2. At the same temperature, CoMoφy873 provided a smaller yield, possibly because of the decrease in the catalyst surface area occurred by the calcination of the precursor at a higher temperature. At higher temperatures, a constant behavior is observed for the selectivity of this catalyst as a function of conversion, within the experimental error. Therefore, the increasing yield obtained with CoMoφy873 with higher temperature is due to the expected increase in conversion with temperature.

Table 2 Catalytic activity of CoMoφy623 and CoMoφy873

Temp. (K)	CoMoφy623			CoMoφy873		
	Selectivity to propene	Conversion	Yield	Selectivity to propene	Conversion	Yield
523	65.3	0.5	0.4			
573	40.5	2.1	0.8			
623	27.9	16.8	4.7	33.6	1.4	0.5
673				32.3	15.4	4.9
723				31.2	17.8	5.6
773				36.5	20.1	7.4
823				35.1	23.4	8.2
873				34.0	25.0	8.5

Catalytic stability of CoMoφy873 was tested at 773 K in continuous reaction for 24 h (see Figure 7) and no loss of catalytic activity was observed. The average conversion value was 20.6%.
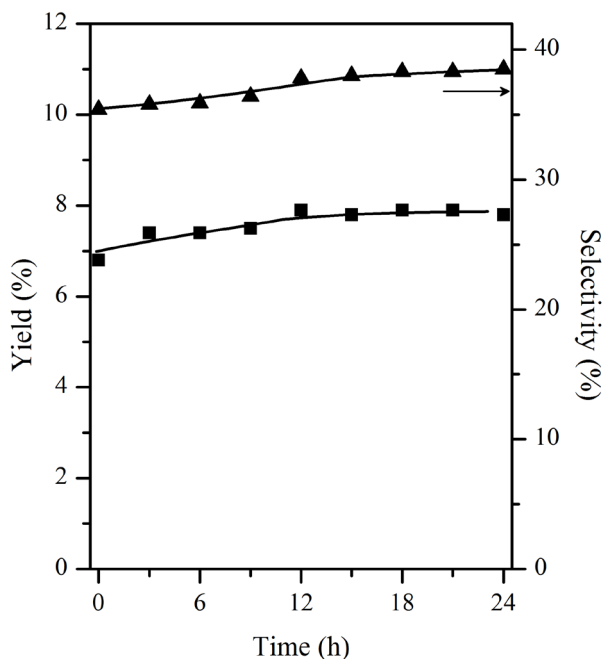
Figure 7 Catalytic stability of CoMoφy873 at 773 K and a space velocity 100 mL g^{-1} min^{-1} yield (-■-) and selectivity (- ▲ -) to propene. The average conversion value was 20.6 %

The main product of the oxidative dehydrogenation of propane is propene; nevertheless, carbon oxides (CO and CO$_2$) are usually formed as by-products via propane and propene combustion. The propane combustion reaction occurs in parallel with ODH; this explains the inability to reach a 100% selectivity to propene [31]. A consecutive oxidation of propene as a function of the temperature can be explained regarding the bond dissociation energy (BDE). The BDE for the methylene hydrogen is 98 kcal mol^{-1} in propane and 88 kcal mol^{-1} in methyl hydrogen in propene [32]; therefore, the transformation of propene to carbon oxides is promoted at higher temperatures. To avoid the oxidation, the propene desorption should be a fast step in the reaction.

The ability of the metal ions to switch between oxidation states, the electronic conductivity of the material, the mobility of lattice oxygen, as well as, the type of oxygen present at the surface are just some of the factors that can affect the activity and selectivity of a catalyst [33]. Even though, a direct comparison of the catalytic activity between CoMoφy623 and CoWsφy673 cannot be made for the differences in the composition and structure. The reducibility can be correlated with the redox capacity of materials, which is necessary for the catalytic activity through a Mars-vans Krevelen mechanism. In our case, CoMoφy623 has a lower onset temperature for the reduction, as

well as, the higher catalytic activity in the temperature range studied. The yields achieved with CoMoφy623 and CoMoφy873, at different temperatures, are comparable to the ones already reported in the literature; the best yield for cobalt-based materials is around 11% [34–36].

Moreover, the difference in the selectivity, Figure 5(b), value between cobalt molybdate and cobalt tungstate could be attributed to the cobalt, it lies in a high spin state in the tungstate, while it is in a low spin state in the molybdate. This is consistent with cobalt forming an inorganic radical (Co–O$_*$) in the tungstate and not in the molybdate, a species highly active in attacking paraffins, improving the velocity of methylene hydrogen abstraction [37].

4. Conclusions

The synthesis method used is suitable to obtain precursors materials for the catalytic oxidative dehydrogenation of propane. The cobalt- molybdenum precursor material was identified as CoMoφy. After calcination of the CoMoφy, the β-CoMoO$_4$ (CoMoφy623 and CoMoφy873) phase was obtained. For the cobalt-tungsten precursor material denominated CoWsφy is a mixture of scheelite-type oxides and wolframite-type oxide according with the FTIR and DRX results. A low crystalline wolframite-type material (CoWsφy673) is obtained after calcination.

The best catalytic activity, based on selectivity to propene and conversion, was observed for CoMoφy623.The good catalytic performance of this material was related to a low onset temperature in the hydrogen reduction profiles. This material was tested at higher temperatures, the selectivity was constant, and the conversion increased. This material is promising for the ODH of propane.

The cobalt-tungsten material is interesting because it exhibited a high selectivity, then it is recommended to study other reaction variables to increase the conversion.

5. Acknowledgments

6. References

1. K. G. Mittal, "Cracking paraffinic hydrocarbons to make alpha olefins—a review," *J. Chem. Technol. Biotechnol.*, vol. 36, no. 7, pp. 291–299, 1986.
2. D. Sanfilippo and I. Miracca, "Dehydrogenation of paraffins: synergies between catalyst design and reactor engineering," *Catal. Today*, vol. 111, no. 1–2, pp. 133–139, 2006.
3. K. Seshan, "Oxidative conversion of lower alkanes to olefins," *Catalysis*, vol. 22, pp. 119–143, 2010.
4. F. Cavani, N. Ballarini, and A. Cericola, "Oxidative dehydrogenation of ethane and propane: How far from

commercial implementation?," *Catal. Today*, vol. 127, no. 1–4, pp. 113–131, 2007.

5. A. F. Wagner, I. R. Slagle, D. Sarzynski, and D. Gutman, "Experimental and theoretical studies of the ethyl + oxygen reaction kinetics," *J. Phys. Chem.*, vol. 94, no. 5, pp. 1853–1868, 1990.

6. C. A. Carrero, R. Schloegl, I. E. Wachs, and R. Schomaecker, "Critical Literature Review of the Kinetics for the Oxidative Dehydrogenation of Propane over Well-Defined Supported Vanadium Oxide Catalysts," *ACS Catal.*, vol. 4, no. 10, pp. 3357–3380, 2014.

7. F. Cavani and F. Trifirò, "The oxidative dehydrogenation of ethane and propane as an alternative way for the production of light olefins," *Catal. Today*, vol. 24, no. 3, pp. 307–313, 1995.

8. H. H. Kung and M. C. Kung, "Oxidative dehydrogenation of alkanes over vanadium-magnesium-oxides," *Appl. Catal. A: Gen.*, vol. 157, no. 1–2, pp. 105–116, 1997.

9. K. Alexopoulos, M. F. Reyniers, and G. B. Marin, "Reaction path analysis of propane selective oxidation over V_2O_5 and V_2O_5/TiO_2," *J. Catal.*, vol. 289, pp. 127–139, 2012.

10. A. Qiao *et al.*, "Oxidative dehydrogenation of ethane to ethylene over V_2O_5/Nb_2O_5 catalysts," *Catal. Commun.*, vol. 30, pp. 45–50, 2013.

11. P. Viparelli *et al.*, "Oxidative dehydrogenation of propane over vanadium and niobium oxides supported catalysts," *Appl. Catal. A: Gen.*, vol. 184, no. 2, pp. 291–301, 1999.

12. X. Fan *et al.*, "Synthesis of a new ordered mesoporous $NiMoO_4$ complex oxide and its efficient catalytic performance for oxidative dehydrogenation of propane," *J. Energy Chem.*, vol. 23, no. 2, pp. 171–178, 2014.

13. B. Pillay, M. R. Mathebula, and H. B. Friedrich, "The oxidative dehydrogenation of n-hexane over Ni–Mo–O catalysts," *Appl. Catal. A: Gen.*, vol. 361, no. 1–2, pp. 57–64, 2009.

14. F. Dury, M. A. Centeno, E. M. Gaigneaux, and P. Ruiz, "An attempt to explain the role of CO_2 and N_2O as gas dopes in the feed in the oxidative dehydrogenation of propane," *Catal. Today*, vol. 81, no. 2, pp. 95–105, 2003.

15. G. Che, R. Quintana, R. S. Ruiz, J. S. Valente, and C. O. Castillo, "Kinetic modeling of the oxidative dehydrogenation of ethane to ethylene over a MoVTeNbO catalytic system," *Chem. Eng. J.*, vol. 252, pp. 75–88, 2014.

16. P. Sazama *et al.*, "Structure and critical function of Fe and acid sites in Fe-ZSM-5 in propane oxidative dehydrogenation with N_2O and N_2O decomposition," *J. Catal.*, vol. 299, pp. 188–203, 2013.

17. M. A. Botavina *et al.*, "Oxidative dehydrogenation of C3–C4 paraffins in the presence of CO_2 over CrO_x/SiO_2 catalysts," *Appl. Catal. A Gen.*, vol. 347, no. 2, pp. 126–132, 2008.

18. M. A. Larrubia J. M. Blasco, L. J. Alemany, and C. Herrera, "Estudio de la catálisis de la deshidrogenación oxidativa del propano: empleo de sistemas catalíticos multimetálicos soportados," *Ing. Química*, vol. 424, pp. 132–144, 2005.

19. B. Solsona *et al.*, "Supported Ni–W–O Mixed Oxides as Selective Catalysts for the Oxidative Dehydrogenation of Ethane," *Top. Catal.*, vol. 52, no. 6–7, pp. 751–757, 2009.

20. M. Salamanca, Y. E. Licea, A. Echavarría, A. C. Faro, and L. A. Palacio, "Hydrothermal synthesis of new wolframite type trimetallic materials and their use in oxidative dehydrogenation of propane," *Phys. Chem. Chem. Phys.*, vol. 11, no. 41, pp. 9583–9591, 2009.

21. B. Farin, M. Devillers, and E. M. Gaigneaux. "Nanostructured hybrid materials as precursors of mesoporous NiMo-based catalysts for the propane oxidative dehydrogenation," *Microporous Mesoporous Mater.*, vol. 242, pp. 200-207, 2017.

22. H. Pezerat, "Problemes de non-stoechiométrie dans certains molybdates hydratés de zinc, cobalt et nickel," *Bull. Soc. Fr. Mineral. Cristallogr.*, vol. 90, pp. 549–552, 1967.

23. D. Levin, S. L. Soled, and J. Y. Ying, "Crystal Structure of an Ammonium Nickel Molybdate Prepared by Chemical Precipitation," *Inorg. Chem.*, vol. 35, no. 14, pp. 4191–4197, 1996.

24. G. W. Smith, "The crystal structures of cobalt molybdate $CoMoO_4$ and nickel molybdate $NiMoO_4$," *Acta Crytallographica*, vol. 15, pp. 1054–1057, 1962.

25. J. Brito and A. L. Barbosa, "Effect of Phase Composition of the Oxidic Precursor on the HDS Activity of the Sulfided Molybdates of Fe(II), Co(II), and Ni(II)," *J. Catal.*, vol. 171, no. 2, pp. 467–475, 1997.

26. M. Suvanto, J. Räty, and T. A. Pakkanen, "Catalytic activity of carbonyl precursor based W/Al_2O_3 and CoW/Al_2O_3 catalysts in hydrodesulfurization of thiophene," *Appl. Catal. A: Gen.*, vol. 181, no. 1, pp. 189–199, 1999.

27. I. Matsuura, S. Mizuno, and H. Hashiba, "Acidic properties of molybdate-based catalysts for propylene oxidation," *Polyhedron*, vol. 5, no. 1–2, pp. 111–117, 1986.

28. A. de Oliveira *et al.*, "Yellow $Zn_xNi_{1-x}WO_4$ pigments obtained using a polymeric precursor method," *Dye. Pigment.*, vol. 77, no. 1, pp. 210–216, 2008.

29. G. M. Clark and W. P. Doyle, "Infra-red spectra of anhydrous molybdates and tungstates," *Spectrochim. Acta*, vol. 22, no. 8, pp. 1441–1447, 1966.

30. S. A. Redfern, "Hard-mode infrared study of the ferroelastic phase transition in $CuWO_4$ - $ZnWO_4$ mixed crystals," *Phys. Rev. B*, vol. 48, no. 9, pp. 5761–5765, 1993.

31. K. Chen, E. Iglesia, and A. T. Bell, "Kinetic Isotopic Effects in Oxidative Dehydrogenation of Propane on Vanadium Oxide Catalysts," *J. Catal.*, vol. 192, no. 1, pp. 197–203, 2000.

32. Y. R. Luo, *Handbook of Bond Dissociation Energies in Organic Compounds*, 1st ed. Florida, USA: CRC Press, 2002.

33. G. Centi, F. Cavani and F. Trifirò, *Selective Oxidation by Heterogeneous Catalysis (Fundamental and Applied Catalysis)*, 1st ed. New York, USA: Springer Science & Business Media, 2001

34. S. Sugiyama, T. Shono, D. Makino, T. Moriga, and H. Hayashi, "Enhancement of the catalytic activities in

propane oxidation and H–D exchangeability of hydroxyl groups by the incorporation with cobalt into strontium hydroxyapatite," *J. Catal.*, vol. 214, no. 1, pp. 8–14, 2003.

35. D. Stern and R. K. Grasselli, "Propane Oxydehydrogenation over Molybdate-Based Catalysts," *J. Catal.*, vol. 167, no. 2, pp. 550–559, 1997.

36. B. Y. Jibril and S. Ahmed, "Oxidative dehydrogenation of propane over Co, Ni and Mo mixed oxides/MCM-41 catalysts: Effects of intra- and extra-framework locations of metals on product distributions," *Catal. Commun.*, vol. 7, no. 12, pp. 990–996, 2006.

37. D. Stern and R. K. Grasselli, "Propane Oxydehydrogenation over Metal Tungstates," *J. Catal.*, vol. 167, no. 2, pp. 570–572, 1997.